

# A Rotation-based Method for Precoding in Gaussian MIMOME Channels

Xinliang Zhang, Yue Qi, and Mojtaba Vaezi, *Senior Member, IEEE*

## Abstract

The problem of maximizing secrecy rate of multiple-input multiple-output multiple-eavesdropper (MIMOME) channels with arbitrary numbers of antennas at each node is studied in this paper. It is proved that linear beamforming is optimum for this problem and optimal signaling to achieve the secrecy capacity is then developed. To this end, it is shown that optimal precoding is a rotation matrix resulted from a set of basic rotations each with one parameter. Next, a gradient-descent based algorithm is developed to find the rotation and power allocation parameters. The proposed rotation-based method can be applied to any MIMOME channels and outperforms state-of-the-art analytical and numerical methods. In particular, the rotation-based precoding achieves higher secrecy rates than the celebrated generalized singular value decomposition (GSVD)-based precoding, with a reasonably higher computational complexity. To further, decrease the computation cost, an algorithm is developed to combine the rotation and GSVD-based precoding. The new rotation-GSVD-based precoding provides an efficient approach to find a near-optimal transmit strategy for the MIMOME channel. Extensive numerical results elaborate on the effectiveness of the rotation-GSVD-based precoding. The new framework developed in this paper can be applied to a verity of similar problems in the context of multi-antenna channels with and without secrecy.

## Index Terms

Physical layer security, MIMO wiretap channel, secrecy capacity, beamforming, precoding, covariance, rotation.

## I. INTRODUCTION

As a complement to higher-layer security measures, *physical layer security* has emerged as a significant technique for security in the lowest layer of communication, i.e., the physical

The authors are with the Department of Electrical and Computer Engineering, Villanova University, PA, USA (e-mail: {xzhang4, yqi, mvaезi}@villanova.edu).

layer. Founded on information theoretic security, which is built on Shannon's notion of perfect secrecy, physical layer security can offer unbreakable security, unlike traditional secret-key-based methods. Physical layer security was laid in the 1970s in Wyner's seminal work on the *wiretap channel* [1] where the idea of secure communication based on the communication channel itself without using encryption keys was first introduced. In this work, Wyner proved that in a wiretap channel (a channel in which a transmitter conveys information to a legitimate receiver in the presence of an eavesdropper) communication can be both robust to transmission errors (*reliable*) and confidential (*secure*), to a certain degree, provided that the legitimate user's channel is better than the eavesdropper's channel.<sup>1</sup> He established the capacity of the *degraded* wiretap channel. Later, Csiszar and Korner [3] generalized this result to arbitrary, not necessarily degraded, wiretap channels.

In the past few decades, physical layer security has been applied to enhance the classical wiretap channel, e.g., by including more realistic assumptions, and to study other wireless channel models. Particularly, as multiple-input multiple-output (MIMO) networks continue to flourish worldwide, significant effort has been applied to the study of MIMO wiretap channels which allow for exploitation of the space/time/user dimensions of wireless channels for secure communications. Specifically, secrecy capacity of Gaussian multiple-input multiple-output multiple-eavesdropper (MIMOME) channels under an average total power constraint was established independently in [4]–[6]. The capacity result is abstracted as an optimization problem over the input covariance matrix. This problem is non-convex and its optimal solution is known only for limited settings [7]–[11].

Among notable sub-optimal solutions that can be applied to the MIMOME channel is the *generalized singular value decomposition* (GSVD)-based precoding of Khisti and Wornell [4]. GSVD-based precoding decomposes transmitted channel matrices into several parallel subchannels and confidential information is transmitted over subchannels where the legitimate user is stronger than the eavesdropper. This method gives a closed-form solution for achievable secrecy rate which is relatively fast and is asymptotically optimal at high signal-to-noise ratios (SNRs). Its performance is, however, not good at certain settings, e.g., when the eavesdropper has a single antenna while other nodes have multiple antennas [11]. Another important sub-optimal solution

<sup>1</sup>Later in the 1990s, Maurer proved that secret key generation through public communication over an insecure yet authenticated channel is possible even when a legitimate user has a worse channel than an eavesdropper [2].

is Li *et. al*'s alternating optimization and water filling (AO-WF) algorithm [12] which alternates the original optimization problem to a convex problem and finds the corresponding Lagrange multipliers in an iterative manner. AO-WF is more computationally expensive than GSVD-based precoding but it can provide a better secrecy rate in some settings. The performance of this method also varies depending on the number of antennas at different nodes. For example, its performance is not as good as the GSVD-based precoding when the number of antennas at the eavesdropper is greater than that of the transmitter. There are also other numerical solutions for this optimization problem. For example, an iterative algorithm with a barrier method is proposed in [13]–[15] to find the covariance matrix.

Recently, based on a new parametrization of the covariance matrix, a closed-form solution for optimal precoding and power allocation of the MIMOME channel with two transmit antennas was obtained in [11], [16]. This approach in finding the optimal covariance matrix is completely different from existing linear beamforming methods. It does not require degradedness condition of [9] and [10], and thus provides the optimal solution for both full-rank and rank-deficient cases in one shot. The proposed beamforming and power allocation schemes are limited to two transmit antenna cases, and optimal transmit covariance matrix is still open in general.

In this paper, we extend the approach of [16] to a MIMOME channel with an arbitrary number of antennas at each node. We establish an optimal precoding and power allocation method named rotation-based method. In this approach, the precoding matrix is formed by a rotation matrix. We take the covariance matrix as an operator to stretch and rotate the input symbols to form a transmit signal that best fits the channels of the legitimate user and eavesdropper. The capacity expression is then transformed to another problem which can be interpreted as finding the maximum area and volume in two and three dimensional coordinate systems and a hypervolume in a higher dimension, depending on the number of transmit antennas. We then solve the new problem and show that it outperforms the existing methods in various antenna settings.

#### A. Contributions

The main contributions of this paper are listed below:

- We introduce a rotation-based parameterization of the covariance matrix and prove that a rotation matrix of size  $n_t$  gives the optimal precoding matrix for the MIMOME channel with  $n_t$  antennas at the transmitter. This new parameterization also reveals that *linear precoding* achieves the capacity of the MIMOME channel.

- For  $n_t = 1$  and  $n_t = 2$ , the proposed scheme reduces to those in [8] and [11], respectively, for which closed-form solutions are known. For  $n_t \geq 3$ , finding a closed-form solution is still challenging. In such a case, we introduce a gradient-based iterative optimization method to determine optimal rotation angles and power allocation parameters. Numerical results in different antenna settings confirm that the proposed scheme works better than the well-known GSVD-based and AO-WF methods. Specifically, the proposed approach outperforms GSVD-based precoding when  $n_e < n_t$ , and AO-WF approach when  $n_e \geq n_t$ , where  $n_e$  is the number of antennas at the eavesdropper. Particularly, the gap between the proposed and GSVD-based methods is remarkably high when the eavesdropper has a single antenna.
- To improve the computational complexity of the proposed algorithm (by reducing the number of iterations), we develop an algorithm to exploit GSVD-based precoding and power allocation as an initial point for our rotation-based approach. The combination of the two approaches, named rotation-GSVD-based approach, improves the results of the both approaches and implies less computational complexity than the rotation-based approach.
- As a byproduct of this work, we improve the performance of the AO-WF algorithm of [12] when  $n_e \geq n_t$ . Under such a circumstance, the first several iterations of AO-WF algorithm does not give a nonzero solution for the Lagrange multiplier, which deteriorates its performance. We fix this issue as elaborated in the simulation results.

It is worth mentioning that, the findings of this paper are directly applicable to MIMO channels without eavesdropper.

### *B. Other Related Works*

An interesting aspect of the developed framework is its generality and its great potential for extension to other related problems. The MIMOME channel has turned out as a fundamental tool for the study of physical-layer security in many other related problems throughout the past decade. The solutions developed for the MIMOME has appeared to be instrumental in designing transmit strategies that maximize secrecy rate of extensions of this basic channel model to MIMO channels with multiple eavesdroppers [12], secure relaying [17], [18], ergodic secrecy rate [19], finite alphabet signaling [20]–[22], multiple access, broadcast, and interference channels [23]–[26], non-orthogonal multiple access channel [27], cognitive radio [28], visible light communication [29], and simultaneous wireless information and power transfer [30]–[32]

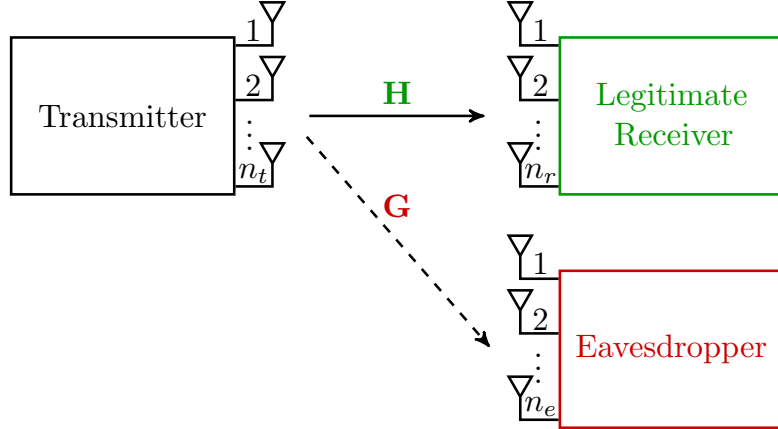


Fig. 1: The MIMOME channel with  $n_t$ ,  $n_r$ , and  $n_e$  antennas at the transmitter, legitimate receiver, and eavesdropper.

among others. Therefore, it is worth studying the optimal covariance matrix of the MIMOME channel as a general tool for physical-layer security in various MIMO settings.

### C. Organizations and Notations

The remainder of this paper is organized as follows. Section II describes the system model and related works. Section III introduces and elaborates on the rotation-based precoding by reformulating the secrecy capacity for the MIMOME channel. Section IV, details a gradient descent based algorithm to optimize the achievable secrecy rate. In Section V numerous simulation results are carried out to demonstrate the effectiveness of the proposed method. Section VI draws the conclusion.

Notations: Bold lowercase letters denote column vectors and bold uppercase letters denote matrices.  $\mathbf{A}(i, j)$  denotes the entry  $(i, j)$  of matrix  $\mathbf{A}$ .  $|\cdot|$ ,  $(\cdot)^T$ ,  $\ln(\cdot)$ ,  $\text{tr}(\cdot)$  denote the absolute value, Euclidean norm, transpose, natural logarithm, respectively.  $\text{diag}(\cdot)$  denotes the diagonal matrix of the set inside.

## II. SYSTEM MODEL AND RELATED WORKS

### A. System Model

We consider a MIMOME channel with  $n_t$  antennas at the transmitter,  $n_r$  antennas at the receiver, and  $n_e$  antennas at the eavesdropper as depicted in Fig. 1. The received signals at the

legitimate receiver and the eavesdropper can be, respectively, expressed as

$$\mathbf{y}_r = \mathbf{H}\mathbf{x} + \mathbf{w}_r, \quad (1a)$$

$$\mathbf{y}_e = \mathbf{G}\mathbf{x} + \mathbf{w}_e, \quad (1b)$$

in which  $\mathbf{H} \in \mathbb{R}^{n_r \times n_t}$  and  $\mathbf{G} \in \mathbb{R}^{n_e \times n_t}$  are the channels corresponding to the receiver and eavesdropper,  $\mathbf{x} \in \mathbb{R}^{n_t}$  is transmitted signal, and  $\mathbf{w}_r \in \mathbb{R}^{n_r}$  and  $\mathbf{w}_e \in \mathbb{R}^{n_e}$  are independent and identically distributed (i.i.d) Gaussian noises with zero means and identity covariance matrices. A representation of secrecy capacity is given by [6]

$$\begin{aligned} \mathcal{C}_s = \max_{\mathbf{Q}} \frac{1}{2} \{ & \log |\mathbf{I}_{n_r} + \mathbf{H}\mathbf{Q}\mathbf{H}^T| - \log |\mathbf{I}_{n_e} + \mathbf{G}\mathbf{Q}\mathbf{G}^T| \} \\ \text{s. t. } & \mathbf{Q} \succeq 0, \mathbf{Q} = \mathbf{Q}^T, \text{tr}(\mathbf{Q}) \leq P_t, \end{aligned} \quad (2)$$

where  $\mathbf{Q} = E\{\mathbf{x}\mathbf{x}^T\} \in \mathbb{R}^{n_t \times n_t}$  is the covariance matrix of the channel input  $\mathbf{x}$  and  $P_t$  is the total transmit power.  $\mathbf{Q}$  is symmetric and positive semi-definite (PSD) by definition.

### B. Existing Results

The optimal transmission over the MIMOME channel is still an open problem in general. However, there are a number of notable analytical results for special numbers of antennas as well as numerical results as listed below.

1) *Analytical Solutions*: An analytical capacity-achieving covariance matrix is known only for special cases. These are limited to:

- $n_t = 1$ : this is the single-input multiple-output (SIMO) case in which  $\mathbf{Q}$  is a scalar and the optimal solution is either  $P_t$  or 0 [8].
- $n_r = 1$ : the so-called multiple-input single-output multiple-eavesdropper (MISOME) channel in which *generalized eigenvalue decomposition* of  $\mathbf{H}$  and  $\mathbf{G}$  achieves the capacity [33].
- $n_t = 2$ ,  $n_r = 2$ , and  $n_e = 1$ : the optimization problem is shown to be the Rayleigh quotient and optimal signaling, which is the maximum eigenvalue of this problem, is unit-rank [7].
- $n_t = 2$ : in which the secrecy capacity is obtained by modeling the covariance matrix as a  $2 \times 2$  rotation matrix [11], [16].
- $\mathbf{Q}$  is full-rank (which implies  $\mathbf{H}^T\mathbf{H} - \mathbf{G}^T\mathbf{G} \succ 0$ ) and also  $P_t$  is greater than a certain threshold [9], [10]: in this case the problem is convex and KarushKuhnTucker (KKT) conditions are used to find the optimal  $\mathbf{Q}$ .

It is worth noting that, as  $n_t$  grows, few channel realizations satisfy the above conditions. For  $n_t = 3$ ,  $n_r = 3$ , and  $n_e = 1$ , for example, the probability that a full-rank solution exist is less than 18.2%.<sup>2</sup> This value decreases when  $n_e$  goes up. Therefore, it can be said that an analytical solution for the MIMOME channel is still an open problem in many practical cases.

2) *Suboptimal Analytical Solution*: For a general MIMOME channel, a sub-optimal solution can be obtained using GSVD-based beamforming [4]. By applying GSVD on  $\mathbf{H}$  and  $\mathbf{G}$ , the optimization problem (2) is simplified to a set of parallel non-interfering channels whose optimal power allocation can be obtained using Lagrange multiplier and KKT conditions [34]. Since parallelization using GSVD does not necessarily convert this problem into an equivalent one, GSVD-based beamforming is not the optimal solution in general. It is not even close enough to the capacity in some cases.

3) *Numerical Solutions*: There are still important cases of the MIMOME for which optimal  $\mathbf{Q}$  is unknown. Due to the intractability of the problem in an analytical form, numerical solutions have been developed to tackle this problem. The alternating optimization water-filling (AO-WF) [12], which is computationally efficient to implement, is one of them. Despite its effectiveness in many cases, AO-WF experiences problems when  $n_e$  is greater than  $n_t$ , for example, which is caused by a failure in finding an optimal Lagrange multiplier. We modify this issue in this paper as we will see later in Section V. The price is a higher time consumption, in the modified approach.

In the next section, we introduce a new model for the covariance matrix  $\mathbf{Q}$  which is a generalization of the solution in [11], [12], from  $n_t = 2$  to any arbitrary  $n_t$ . This model is then used to find transmit signaling that can be used to achieve secrecy capacity of the MIMOME channel regardless of the number of antennas at different nodes.

### III. A ROTATION-BASED MODELING OF THE PROBLEM

The secrecy capacity of the MIMOME channel in (2) can be rewritten as [11]

$$\mathcal{C}_s = \max_{\mathbf{Q} \succeq 0, \text{tr}(\mathbf{Q}) \leq P_t} \frac{1}{2} \log \frac{|\mathbf{I}_{n_t} + \mathbf{H}^T \mathbf{H} \mathbf{Q}|}{|\mathbf{I}_{n_e} + \mathbf{G}^T \mathbf{G} \mathbf{Q}|}. \quad (3)$$

<sup>2</sup>This is obtained by Monte Carlo experiments with  $10^6$  trials where  $\mathbf{H}$  and  $\mathbf{G}$  have the same distributions.

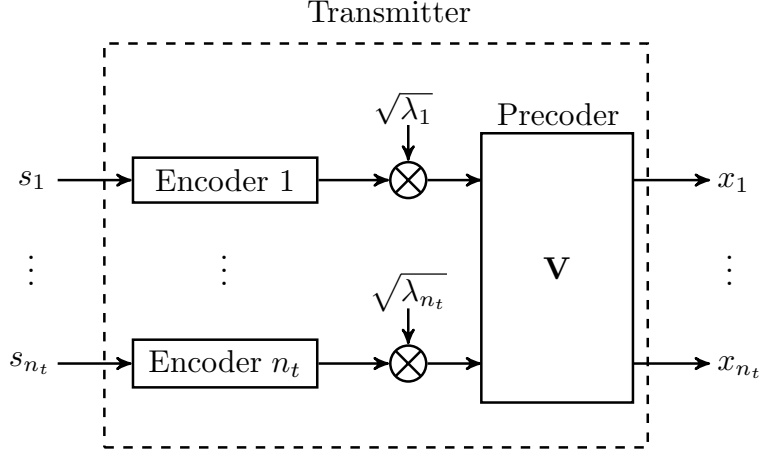


Fig. 2: The structure of the proposed linear precoding and power allocation.

Also, the covariance matrix  $\mathbf{Q}$  can be eigendecomposed as

$$\mathbf{Q} = \mathbf{V} \Lambda \mathbf{V}^T, \quad (4)$$

in which  $\Lambda$  is a diagonal matrix and its diagonal elements are the eigenvalues of  $\mathbf{Q}$ , which are real and non-negative, i.e.,

$$\Lambda = \text{diag}(\lambda_i), \quad \lambda_i \geq 0, \quad i = 1, 2, \dots, n_t, \quad (5)$$

and  $\mathbf{V} \in \mathbb{R}^{n_t \times n_t}$  is the matrix composed of  $n_t$  corresponding eigenvectors of  $\mathbf{Q}$  in  $\mathbb{R}^{n_t}$  vector space. With this, the total power constraint  $\text{tr}(\mathbf{Q}) \leq P_t$  will be equivalent to

$$\sum_{i=1}^{n_t} \lambda_i \leq P_t. \quad (6)$$

An immediate implication of the above decomposition is that linear precoding can achieve the capacity of the MIMOME channel. The architecture of the above linear precoding and power allocation is depicted in Fig. 2. In this figure,  $s_1, \dots, s_{n_t}$  are input symbols which are independent and identically distributed Gaussian random variables with zero means and unit variances,  $\lambda_i$ s are power allocation coefficients,  $\mathbf{V}$  is the precoding matrix, and  $\mathbf{x} = [x_1, \dots, x_{n_t}]^T$  is the transmit vector whose covariance is  $\mathbf{Q}$ . Since  $\mathbf{Q}$  is symmetric, the matrix  $\mathbf{V}$  is *orthonormal*. Then it can be considered as a rotation operation applied to the vector multiplied with (see, Fig. 2). Because of this, we use a series of *basic rotation* matrices to represent the orthonormal matrix  $\mathbf{V}$ . Each

basic rotation matrix represents the rotation between two axes in  $\mathbb{R}^{n_t}$  vector space while other axes are fixed. In the following subsections, we first review the rotation-based method for  $n_t = 2$  and then generalize it to  $n_t = 3$  and arbitrary  $n_t$ .

#### A. Rotation-based Method for $n_t = 2$ [16]

The capacity region of MIMOME channel with two transmit antennas has been established in [11], [16], using a rotation matrix in two-dimensional (2D) space. In this case, eigenvalue matrix  $\Lambda$  can be written as

$$\Lambda = \begin{bmatrix} \lambda_1 & 0 \\ 0 & \lambda_2 \end{bmatrix}, \quad (7)$$

and, without loss of generality, the eigenvectors can be written as the following orthonormal (rotation) matrix

$$\mathbf{V} = \mathbf{V}_{12} = \begin{bmatrix} \cos \theta_{12} & -\sin \theta_{12} \\ \sin \theta_{12} & \cos \theta_{12} \end{bmatrix}. \quad (8)$$

The parameter  $\theta_{12}$  in rotation matrix  $\mathbf{V}_{12}$  is the rotation angle corresponding to the rotation from the direction of the standard basis (unit vector)  $\mathbf{e}_1 = (1, 0)^T$  to the standard basis  $\mathbf{e}_2 = (0, 1)^T$  in  $\mathbb{R}^2$  vector space. This rotation is achieved on the plane defined by  $\mathbf{e}_1$  and  $\mathbf{e}_2$ . Then, the covariance matrix  $\mathbf{Q}$  can be built using three parameters: the two non-negative eigenvalues  $\lambda_1$  and  $\lambda_2$ , and the rotation angle  $\theta_{12}$ . With these parameters, we can represent any arbitrary  $2 \times 2$  covariance matrix as in (4). Then the original optimization problem can be equivalently converted to

$$\mathcal{C}_s = \max_{\lambda_1, \lambda_2, \theta_{12}} \frac{1}{2} \log \frac{|\mathbf{I}_{n_t} + \mathbf{H}^T \mathbf{H} \mathbf{V} \Lambda \mathbf{V}^T|}{|\mathbf{I}_{n_t} + \mathbf{G}^T \mathbf{G} \mathbf{V} \Lambda \mathbf{V}^T|}, \quad (9a)$$

$$\text{s. t. } \lambda_1 \geq 0, \lambda_2 \geq 0, \lambda_1 + \lambda_2 \leq P_t. \quad (9b)$$

In the light of this modeling, an analytical solution for optimal precoding matrix and power allocation scheme according to  $\Lambda$  are obtained in [16] by finding  $\theta_{12}$ ,  $\lambda_1$  and  $\lambda_2$ . In the next subsection, we extend this method to the cases with  $n_t = 3$ .

### B. Rotation-based Method for $n_t = 3$

Similar to the previous case, we use the eigenvalue decomposition of (4). For  $n_t = 3$ , the eigenvalue matrix  $\Lambda$  can be written as

$$\Lambda = \begin{bmatrix} \lambda_1 & 0 & 0 \\ 0 & \lambda_2 & 0 \\ 0 & 0 & \lambda_3 \end{bmatrix}, \quad (10)$$

in which  $\lambda_i \geq 0$ ,  $i = 1, 2, 3$ . Similarly, the orthonormal matrix  $\mathbf{V}$  can be written as a rotation matrix, which is obtained by a product of three basic rotation matrices,

$$\mathbf{V} = \mathbf{V}_{12}\mathbf{V}_{13}\mathbf{V}_{23}, \quad (11)$$

in which

$$\mathbf{V}_{12} = \begin{bmatrix} \cos \theta_{12} & -\sin \theta_{12} & 0 \\ \sin \theta_{12} & \cos \theta_{12} & 0 \\ 0 & 0 & 1 \end{bmatrix}, \quad (12a)$$

$$\mathbf{V}_{13} = \begin{bmatrix} \cos \theta_{13} & 0 & -\sin \theta_{13} \\ 0 & 1 & 0 \\ \sin \theta_{13} & 0 & \cos \theta_{13} \end{bmatrix}, \quad (12b)$$

and

$$\mathbf{V}_{23} = \begin{bmatrix} 1 & 0 & 0 \\ 0 & \cos \theta_{23} & -\sin \theta_{23} \\ 0 & \sin \theta_{23} & \cos \theta_{23} \end{bmatrix}. \quad (12c)$$

**Lemma 1.** *To reach secrecy capacity of the MIMOME channel with  $n_t = 3$  it is sufficient to use a diagonal  $\Lambda$  and the rotation matrix  $\mathbf{V}$  given in (11) to generate the input covariance matrix  $\mathbf{Q} = \mathbf{V}\Lambda\mathbf{V}^T$ .*

*Proof.* To prove Lemma 1, we first prove  $\mathbf{V}\Lambda\mathbf{V}^T$  is a covariance matrix. Since  $\mathbf{V}_{12}$ ,  $\mathbf{V}_{13}$ , and  $\mathbf{V}_{23}$  are orthonormal matrices, then

$$\mathbf{V}\mathbf{V}^T = \mathbf{V}_{12}\mathbf{V}_{13}\mathbf{V}_{23}\mathbf{V}_{23}^T\mathbf{V}_{13}^T\mathbf{V}_{12}^T = \mathbf{I}, \quad (13)$$

which means  $\mathbf{V}$  is orthonormal. Therefore, if  $\lambda_i \geq 0, \forall i \in \{1, 2, 3\}$  is satisfied, then  $\mathbf{Q}$  is symmetric and PSD, i.e., it is a covariance matrix.

We next prove that any  $3 \times 3$  covariance matrix can be written as (4) in which  $\mathbf{V}$  is a rotation matrix. To this end, it is sufficient to show that any orthonormal matrix  $\mathbf{V}$  can be decomposed as in (11). That is, for any orthonormal matrix  $\mathbf{V}$  we can find a set of  $\theta_{12}$ ,  $\theta_{13}$ , and  $\theta_{23}$ . The rotation angles are obtained in [35]. We state the result here.

- If  $\mathbf{V}(3, 1) \neq \pm 1$ ,

$$\theta_{13} = \arcsin(\mathbf{V}(3, 1)) \text{ or } \theta_{13} = \pi - \arcsin(\mathbf{V}(3, 1)), \quad (14a)$$

$$\theta_{12} = \text{atan2}\left(\frac{\mathbf{V}(2, 1)}{\cos(\theta_{13})}, \frac{\mathbf{V}(1, 1)}{\cos(\theta_{13})}\right), \quad (14b)$$

and

$$\theta_{23} = \text{atan2}\left(\frac{\mathbf{V}(3, 2)}{\cos(\theta_{13})}, \frac{\mathbf{V}(3, 3)}{\cos(\theta_{13})}\right), \quad (14c)$$

in which  $\text{atan2}(\cdot, \cdot)$  is the four-quadrant inverse tangent which is defined as

$$\text{atan2}(x, y) = \begin{cases} \arctan\left(\frac{y}{x}\right), & \text{if } x > 0, \\ \arctan\left(\frac{y}{x}\right) + \pi, & \text{if } x < 0 \text{ and } y \geq 0, \\ \arctan\left(\frac{y}{x}\right) - \pi, & \text{if } x < 0 \text{ and } y < 0, \\ \frac{\pi}{2}, & \text{if } x = 0 \text{ and } y > 0, \\ -\frac{\pi}{2}, & \text{if } x = 0 \text{ and } y < 0, \\ \text{undefined}, & \text{if } x = 0 \text{ and } y = 0. \end{cases} \quad (15)$$

- If  $\mathbf{V}(3, 1) = 1$ , then  $\theta_{12}$  is an arbitrary number ( $\theta_{12} \in \mathbb{R}$ ) and

$$\theta_{13} = \pi/2, \quad (16a)$$

$$\theta_{23} = \theta_{12} + \text{atan2}(\mathbf{V}(1, 2), \mathbf{V}(1, 3)). \quad (16b)$$

- If  $\mathbf{V}(3, 1) = -1$ , then  $\theta_{12}$  is an arbitrary number ( $\theta_{12} \in \mathbb{R}$ ) and

$$\theta_{13} = -\pi/2, \quad (17a)$$

$$\theta_{23} = -\theta_{12} + \text{atan2}(-\mathbf{V}(1, 2), -\mathbf{V}(1, 3)). \quad (17b)$$

Therefore, an arbitrary  $3 \times 3$  covariance matrix can be represented as  $\mathbf{Q} = \mathbf{V}\Lambda\mathbf{V}^T$  where  $\Lambda$  and  $\mathbf{V}$  are defined in (10) and (11).<sup>3</sup> In some scenarios, the eigenvalue decomposition can give us

<sup>3</sup>From the above solution, it is obvious that the solution is not unique.

an improper rotation matrix [36], i.e., an orthonormal matrix whose determinate is  $-1$ . In order to use (11) to find the rotation angles, two eigenvectors of  $\mathbf{V}$  and the corresponding eigenvalues of  $\Lambda$  should be exchanged to ensure  $\det(\mathbf{V}) = 1$ . In such a case, for example, we can define  $\mathbf{V}' = \mathbf{V}\mathbf{I}'$  and  $\Lambda' = \mathbf{I}'^T\Lambda\mathbf{I}'$ , where

$$\mathbf{I}' = \begin{bmatrix} 1 & 0 & 0 \\ 0 & 0 & 1 \\ 0 & 1 & 0 \end{bmatrix}. \quad (18)$$

$\mathbf{I}'$  exchanges the second and third columns of  $\mathbf{V}$  and  $\Lambda$ . But  $\mathbf{Q}$  still can be represented by  $\mathbf{V}'$  and  $\Lambda'$ , since  $\mathbf{I}'\mathbf{I}'^T = \mathbf{I}$  and

$$\mathbf{V}'\Lambda'\mathbf{V}'^T = (\mathbf{V}\mathbf{I}')(\mathbf{I}'^T\Lambda\mathbf{I}')(\mathbf{V}\mathbf{I}')^T = \mathbf{V}\Lambda\mathbf{V}^T. \quad (19)$$

This completes the proof of Lemma 1.  $\square$

Similar to the case with  $n_t = 2$ ,  $\theta_{ij}$  denotes a rotation from the direction of the  $i$ th to the  $j$ th standard basis vectors in  $\mathbb{R}^3$  vector space, where  $i, j \in \{1, 2, 3\}$  and  $i < j$ .

Then, the equivalent optimization problem for  $n_t = 3$  is

$$\mathcal{C}_s = \max_{\Lambda, \theta_{12}, \theta_{13}, \theta_{23}} \frac{1}{2} \log \frac{|\mathbf{I}_{n_t} + \mathbf{H}^T \mathbf{H} \mathbf{V} \Lambda \mathbf{V}^T|}{|\mathbf{I}_{n_t} + \mathbf{G}^T \mathbf{G} \mathbf{V} \Lambda \mathbf{V}^T|}, \quad (20a)$$

$$\text{s. t. } \lambda_i \geq 0, i \in \{1, 2, 3\}; \sum_{i=1}^3 \lambda_i \leq P_t. \quad (20b)$$

### C. Generalization to an Arbitrary $n_t$

To generalize the rotation-based method to an arbitrary  $n_t \times n_t$  covariance matrix, we prove that  $\Lambda \in \mathbb{R}^{n_t \times n_t}$  is a diagonal matrix with non-negative elements  $\Lambda(i, i) = \lambda_i$ , and  $\mathbf{V}$  is a rotation matrix in  $\mathbb{R}^{n_t \times n_t}$  vector space which can be obtained by

$$\mathbf{V} = \prod_{i=1}^{n_t-1} \prod_{j=i+1}^{n_t} \mathbf{V}_{ij}, \quad (21)$$

in which the basic rotation matrix  $\mathbf{V}_{ij}$  is the Givens matrix [37] defined as

$$\mathbf{V}_{ij} = \begin{bmatrix} 1 & \cdots & & \cdots & 0 \\ \vdots & \ddots & & & \vdots \\ & v_{ii} & \cdots & v_{ij} & \vdots \\ & \vdots & \ddots & \vdots & \vdots \\ & v_{ji} & \cdots & v_{jj} & \vdots \\ \vdots & & & \ddots & \vdots \\ 0 & \cdots & & \cdots & 1 \end{bmatrix}, \quad (22)$$

and

$$\begin{bmatrix} v_{ii} & v_{ij} \\ v_{ji} & v_{jj} \end{bmatrix} = \begin{bmatrix} \cos \theta_{ij} & -\sin \theta_{ij} \\ \sin \theta_{ij} & \cos \theta_{ij} \end{bmatrix}. \quad (23)$$

$\mathbf{V}_{ij}$  represents a rotation from the  $i$ th standard basis to the  $j$ th standard basis in  $\mathbb{R}^{n_t}$  vector space with a rotation angle  $\theta_{ij}$ . That is, we show that an arbitrary orthogonal matrix  $\mathbf{V}$  can be represented by (21). Further, an arbitrary covariance matrix  $\mathbf{Q} \in \mathbb{R}^{n_t \times n_t}$  can be represented by  $n_t$  non-negative eigenvalues and  $\frac{1}{2}n_t(n_t - 1)$  rotation angles.

It should be noted that the order of multiplication in (21) is not unique and different order will lead to different rotation angles  $\theta_{ij}$ . In this paper, without loss of generality, we use the order definition in (21).

**Theorem 1.** *To reach the secrecy capacity of the MIMOME with  $n_t \geq 2$  it suffices to use the rotation matrix  $\mathbf{V}$  of (21) as a precoding matrix.*

*Proof.* The proof of Theorem 1 is similar to the proof of Lemma 1. First, it is straightforward to check that  $\mathbf{V}$  in (21) is an orthonormal matrix, as we did in (13). Next, we prove that an arbitrary orthonormal matrix  $\mathbf{V}$  can be written as (21). Equivalently, we may show that

$$\left( \prod_{i=1}^{n_t-1} \prod_{j=i+1}^{n_t} \mathbf{V}_{ij} \right)^T \mathbf{V} = \mathbf{I}. \quad (24)$$

To this end, for a given orthonormal  $\mathbf{V}$ , it suffices to find  $\theta_{ij}$  such that (24) holds. This process is carried out in Algorithm 1. In fact, if we expand the product of matrices on the left side of  $\mathbf{V}$  in (24), we see that  $\mathbf{V}$  is initially multiplied with  $\mathbf{V}_{12}^T$ . Then, the corresponding rotation angle  $\theta_{12}$  can be chosen to set the entry (2, 1) of  $\mathbf{V}$  to zero. Next,  $\mathbf{V}_{13}^T$  is multiplied to the new  $\mathbf{V}$  and  $\theta_{13}$  can be chosen to set the entry (3, 1) to zero. This process continues until the last element

---

**Algorithm 1** Rotation Angles Solution

---

```

1: Initialize  $[\mathbf{V}, \Lambda] = \text{eig}(\mathbf{Q})$ ,  $i = 1$ ;
2: if  $\det(\mathbf{V}) = -1$  then
3:   Exchange first two columns of  $\mathbf{V}$ ;
4:   Exchange first two values on diagonal of  $\Lambda$ ;
5: end if
6: while  $i \leq (n_t - 1)$  do
7:    $j = i + 1$ ;
8:   while  $j \leq n_t$  do
9:      $\theta_{ij} = -\text{atan2}(-\mathbf{V}(j, i), \mathbf{V}(i, i))$ ;
10:     $\mathbf{V}_{\text{rot}} = \mathbf{I}_{n_t}$ ;
11:     $\mathbf{V}_{\text{rot}}(i, i) = \mathbf{V}_{\text{rot}}(j, j) = \cos \theta_{ij}$ ;
12:     $\mathbf{V}_{\text{rot}}(j, i) = -\mathbf{V}_{\text{rot}}(i, j) = \sin \theta_{ij}$ ;
13:     $\mathbf{V} = \mathbf{V}_{\text{rot}} \mathbf{V}$ ;
14:     $j = j + 1$ ;
15:  end while
16:   $i = i + 1$ ;
17: end while
18: Output  $\theta_{ij}$ ,  $\forall 1 \leq i < j \leq n_t$ .

```

---

under the main diagonal of  $\mathbf{V}$ , i.e., the entry  $(n_t, n_t - 1)$ , becomes zero. We note that, since  $\mathbf{V}$  is orthonormal, the upper triangle also will be zero throughout this process. That is, the left side of (24) becomes a unity matrix. This proves Theorem 1. The rotation angles  $\theta_{ij}$  can be obtained by Algorithm 1 which is a generalization of Algorithm 5.1.3 of [37] for vectors in  $\mathbb{R}^{n_t}$ .

□

**Theorem 2.** For ant  $n_t$ , the optimization problem (3) can be equivalently reformulated as

$$\mathcal{C}_s = \max_{\Lambda, \theta_{ij}} \frac{1}{2} \log \frac{|\mathbf{I}_{n_t} + \mathbf{H}^T \mathbf{H} \mathbf{V} \Lambda \mathbf{V}^T|}{|\mathbf{I}_{n_t} + \mathbf{G}^T \mathbf{G} \mathbf{V} \Lambda \mathbf{V}^T|}, \quad (25a)$$

$$\text{s. t. } \lambda_i \geq 0, i \in \{1, \dots, n_t\}; \sum_{i=1}^{n_t} \lambda_i \leq P_t. \quad (25b)$$

This new representation replaces the constraint  $\mathbf{Q} \succeq 0$  by a set of scalar constraints on eigenvalues. Then, numerical methods such as gradient descent can be applied to optimize the parameters  $\theta_{ij}$  and  $\lambda_i$  to maximize (25a) to obtain the optimal secrecy rate.

#### IV. SOLVING THE NEW OPTIMIZATION PROBLEM

The rotation-based construction of  $\mathbf{Q}$  ensures  $\mathbf{Q}$  is symmetric and PSD. For  $\mathbf{Q}$  with dimension  $n_t$ , the required number of parameters is  $\frac{1}{2}n_t(n_t + 1)$ , which is equal to the free variables in  $\mathbf{Q}$ . The rotation-based method can provide a systematic structure to traverse  $\mathbf{Q}$  by traversing a group of parameters which are in finite ranges. The possible range of each  $\theta_{ij}$  in (22) is  $[0, 2\pi]$ .<sup>4</sup> The range of each  $\lambda_i$  is  $[0, P_t]$  with the constraint that sum of all  $\lambda_i$ s should not exceed the average power  $P_t$ . The rotation-based method simplifies the matrix constraints of (2) to scalar constraints in (25b). The eigenvalues in the rotation-based method are power allocation coefficients whereas the rotation matrix acts as the precoding matrix.

The problem is not convex if no constraint is applied to  $\mathbf{H}$  and  $\mathbf{G}$  [10]. However, applying the rotation-based method, the values of local optimums are very close to the global one. The reason is that, a certain covariance matrix  $\mathbf{Q}$  can correspond to different groups of rotation angles and eigenvalues. For example,  $\mathbf{Q}$  will not be changed if we swap  $i$ th and  $j$ th eigenvalues in  $\Lambda$  and  $i$ th and  $j$ th eigenvectors in  $\mathbf{V}$ , whereas, the rotation angles and the order of eigenvalues will change. Moreover, multiple solutions may be caused by the periodicity of angles and no sequencing limitation on eigenvalues. Therefore, some symmetries exist when  $\mathbf{Q}$  is written as a function of  $\theta_{ij}$ s and  $\lambda_i$ s.

For  $n_t = 2$ , a closed-form solution has been obtained in [11]. In this paper, we consider the case with  $n_t \geq 3$ . Since finding analytical solution of  $\lambda_i$  and  $\theta_{ij}$  is challenging, we resort to numerical methods to optimize (25a) and (25b). More specifically, *gradient descent* is applied to find the solution. The gradient descent can be applied to determine the eigenvalues and rotation angles. The gradient descent we use contains two steps: first, we apply gradient descent on eigenvalues for given rotation angles; then, we fix the eigenvalues and apply gradient descent on rotation angles. We then iterate this process. The details are discussed in the following.

<sup>4</sup>It can be proved that in some cases the optimal  $\theta_{ij}$  is in  $[0, \pi)$ . See, for example, the case for  $n_t = 2$  [11].

### A. Gradient Descent-based Solution

We derive the gradient of (25a) with respect to  $\theta_{ij}$  and  $\lambda_i$  in this subsection. By multiplying the nominator and denominator of the argument of the logarithm by  $\mathbf{V}^T$  and  $\mathbf{V}$ , the objective function (25a) can be represented as

$$R(\boldsymbol{\lambda}, \boldsymbol{\theta}) \triangleq \frac{1}{2} \log \frac{|\mathbf{I}_{n_t} + \mathbf{V}^T \mathbf{H}^T \mathbf{H} \mathbf{V} \boldsymbol{\Lambda}|}{|\mathbf{I}_{n_t} + \mathbf{V}^T \mathbf{G}^T \mathbf{G} \mathbf{V} \boldsymbol{\Lambda}|}, \quad (26)$$

in which the  $\boldsymbol{\lambda}$  is the diagonal of  $\boldsymbol{\Lambda}$  and  $\boldsymbol{\theta}$  contains all rotation angles required in  $\mathbf{V}$ .

We first derive the gradient with respect to  $\theta_{ij}$ . For simplicity of presentation, we define

$$\mathbf{A} \triangleq \mathbf{V}^T \mathbf{H}^T \mathbf{H} \mathbf{V} \boldsymbol{\Lambda}, \quad (27a)$$

$$\mathbf{B} \triangleq \mathbf{V}^T \mathbf{G}^T \mathbf{G} \mathbf{V} \boldsymbol{\Lambda}. \quad (27b)$$

We use the Jacobi's formula [38] to calculate the gradient of the determinant of matrix  $\mathbf{M}$

$$\frac{d}{dt} |\mathbf{M}| = |\mathbf{M}| \text{tr} \left( \mathbf{M}^{-1} \frac{d\mathbf{M}}{dt} \right). \quad (28)$$

Then,

$$\frac{d}{dt} \log |\mathbf{M}| = \frac{1}{\ln 2} \text{tr} \left( \mathbf{M}^{-1} \frac{d\mathbf{M}}{dt} \right). \quad (29)$$

The derivative with respect to the rotation angle  $\theta_{ij}$  is

$$\begin{aligned} \frac{\partial R}{\partial \theta_{ij}} &= \frac{\partial}{\partial \theta_{ij}} \frac{1}{2} \log \frac{|\mathbf{I} + \mathbf{A}|}{|\mathbf{I} + \mathbf{B}|} \\ &= \frac{\partial}{\partial \theta_{ij}} \frac{1}{2} \log |\mathbf{I} + \mathbf{A}| - \frac{d}{d\theta_{ij}} \frac{1}{2} \log |\mathbf{I} + \mathbf{B}| \\ &= \eta \cdot \text{tr} \left[ (\mathbf{I} + \mathbf{A})^{-1} \frac{\partial (\mathbf{I} + \mathbf{A})}{\partial \theta_{ij}} \right] - \eta \cdot \text{tr} \left[ (\mathbf{I} + \mathbf{B})^{-1} \frac{\partial (\mathbf{I} + \mathbf{B})}{\partial \theta_{ij}} \right] \\ &= \eta \cdot \text{tr} \left[ (\mathbf{I} + \mathbf{A})^{-1} \frac{\partial \mathbf{A}}{\partial \theta_{ij}} \right] - \eta \cdot \text{tr} \left[ (\mathbf{I} + \mathbf{B})^{-1} \frac{\partial \mathbf{B}}{\partial \theta_{ij}} \right], \end{aligned} \quad (30)$$

where  $\eta = 1/(2 \ln 2)$  and the third equality is due to (29). Next, we get the derivative of  $\mathbf{A}$  with respect to  $\theta_{ij}$ , which is given as

$$\begin{aligned}
\frac{\partial \mathbf{A}}{\partial \theta_{ij}} &= \frac{\partial (\mathbf{V}^T \mathbf{H}^T \mathbf{H} \mathbf{V} \boldsymbol{\Lambda})}{\partial \theta_{ij}} \\
&= \frac{\partial}{\partial \theta_{ij}} \left[ \left( \prod_{m=1}^{n-1} \prod_{k=m+1}^n \mathbf{V}_{mk} \right)^T \mathbf{H}^T \mathbf{H} \left( \prod_{m=1}^{n-1} \prod_{k=m+1}^n \mathbf{V}_{mk} \right) \boldsymbol{\Lambda} \right] \\
&= \left[ \mathbf{V}_\alpha \left( \prod_{k=i+1}^{j-1} \mathbf{V}_{ik} \right) \frac{\partial \mathbf{V}_{ij}}{\partial \theta_{ij}} \left( \prod_{k=j+1}^n \mathbf{V}_{ik} \right) \mathbf{V}_\beta \right]^T \mathbf{H}^T \mathbf{H} \mathbf{V} \boldsymbol{\Lambda} \\
&\quad + \mathbf{V}^T \mathbf{H}^T \mathbf{H} \mathbf{V}_\alpha \left( \prod_{k=i+1}^{j-1} \mathbf{V}_{ik} \right) \frac{\partial \mathbf{V}_{ij}}{\partial \theta_{ij}} \left( \prod_{k=j+1}^n \mathbf{V}_{ik} \right) \mathbf{V}_\beta \boldsymbol{\Lambda},
\end{aligned} \tag{31}$$

where

$$\mathbf{V}_\alpha = \prod_{m=1}^{i-1} \prod_{k=m+1}^n \mathbf{V}_{mk}, \tag{32a}$$

$$\mathbf{V}_\beta = \prod_{m=i+1}^{n-1} \prod_{k=m+1}^n \mathbf{V}_{mk}. \tag{32b}$$

As an example, for  $n_t = 3$  and  $\theta_{ij} = \theta_{23}$  the derivative of  $\mathbf{A}$  is

$$\begin{aligned}
\frac{\partial \mathbf{A}}{\partial \theta_{23}} &= \frac{\partial (\mathbf{V}_{23}^T \mathbf{V}_{13}^T \mathbf{V}_{12}^T \mathbf{H}^T \mathbf{H} \mathbf{V}_{12} \mathbf{V}_{13} \mathbf{V}_{23} \boldsymbol{\Lambda})}{\partial \theta_{23}} \\
&= \frac{d\mathbf{V}_{23}^T}{d\theta_{23}} \mathbf{V}_{13}^T \mathbf{V}_{12}^T \mathbf{H}^T \mathbf{H} \mathbf{V}_{12} \mathbf{V}_{13} \mathbf{V}_{23} \boldsymbol{\Lambda} + \mathbf{V}_{23}^T \mathbf{V}_{13}^T \mathbf{V}_{12}^T \mathbf{H}^T \mathbf{H} \mathbf{V}_{12} \mathbf{V}_{13} \frac{d\mathbf{V}_{23}}{d\theta_{23}} \boldsymbol{\Lambda}.
\end{aligned} \tag{33}$$

Second, we derive the partial derivative with respect to the eigenvalues. The derivative of (26) with respect to  $\lambda_i$  is

$$\begin{aligned}
\frac{\partial R}{\partial \lambda_i} &= \frac{\partial}{\partial \lambda_i} \frac{1}{2} \log \frac{|\mathbf{I} + \mathbf{A}|}{|\mathbf{I} + \mathbf{B}|} \\
&= \rho \cdot \text{tr} \left[ (\mathbf{I} + \mathbf{A})^{-1} \frac{\partial \boldsymbol{\Lambda}}{\partial \lambda_i} \right] - \rho \cdot \text{tr} \left[ (\mathbf{I} + \mathbf{B})^{-1} \frac{\partial \boldsymbol{\Lambda}}{\partial \lambda_i} \right] \\
&= \rho \cdot \text{tr} \left[ (\mathbf{I} + \mathbf{A})^{-1} \mathbf{V}^T \mathbf{H}^T \mathbf{H} \mathbf{V} \frac{\partial \boldsymbol{\Lambda}}{\partial \lambda_i} \right] - \rho \cdot \text{tr} \left[ (\mathbf{I} + \mathbf{B})^{-1} \mathbf{V}^T \mathbf{G}^T \mathbf{G} \mathbf{V} \frac{\partial \boldsymbol{\Lambda}}{\partial \lambda_i} \right],
\end{aligned} \tag{34}$$

in which

$$\frac{\partial \boldsymbol{\Lambda}}{\partial \lambda_i} = \begin{cases} 1, & \text{entry}(i, i), \\ 0, & \text{elsewhere.} \end{cases} \tag{35}$$

To satisfy the constraints in (25b), we need to make sure all eigenvalues are positive and their sum is not greater than  $P_t$ . To satisfy the former we define  $\boldsymbol{\lambda}^+ = \max\{0, \boldsymbol{\lambda}\}$  make the negative

elements of  $\boldsymbol{\lambda}$  zero. For the latter, we add a penalty function on eigenvalues after each step of its gradient descent. Specifically, we let

$$\boldsymbol{\lambda} = P_t \frac{\boldsymbol{\lambda}^+}{\sum_{i=1}^{n_t} \lambda_i^+}. \quad (36)$$

So far we have the gradient of (26) with respect to eigenvalues and rotation angles as follow

$$\nabla_{\boldsymbol{\theta}} R = \left[ \frac{\partial R}{\partial \theta_{12}}, \dots, \frac{\partial R}{\partial \theta_{ij}}, \dots, \frac{\partial R}{\partial \theta_{(n_t-1)n_t}} \right], \quad (37a)$$

$$\nabla_{\boldsymbol{\lambda}} R = \left[ \frac{\partial R}{\partial \lambda_1}, \dots, \frac{\partial R}{\partial \lambda_{n_t}} \right]. \quad (37b)$$

### B. Initialization of the Gradient Descent

The gradient (26) with respect to both rotation angles and eigenvalues have many repetitive factors that can reduce computation time. Besides, efficient initial values can further reduce the iteration time. A feasible way is to initialize the algorithm is to use GSVD-based beamforming [34] for  $\mathbf{Q}$ . The solution given by GSVD-based beamforming provides a precoding matrix  $\mathbf{E}$  which satisfy

$$\mathbf{H}\mathbf{E} = \boldsymbol{\Psi}_r \mathbf{C}, \quad (38a)$$

$$\mathbf{G}\mathbf{E} = \boldsymbol{\Psi}_e \mathbf{D}, \quad (38b)$$

$$\mathbf{C}^T \mathbf{C} + \mathbf{D}^T \mathbf{D} = \mathbf{I}, \quad (38c)$$

where  $\mathbf{E} \in \mathbb{R}^{n_t \times q}$ ,  $q = \min(n_t, n_r + n_e)$ ,  $\mathbf{C}^T \mathbf{C} = \text{diag}(c_i)$  and  $\mathbf{D}^T \mathbf{D} = \text{diag}(d_i)$ ,  $i \in \{1, \dots, q\}$ , are diagonal matrices, and  $\boldsymbol{\Psi}_r \in \mathbb{R}^{n_r \times n_r}$  and  $\boldsymbol{\Psi}_e \in \mathbb{R}^{n_e \times n_e}$  are orthonormal matrices. Besides, the power allocation matrix  $\mathbf{P} = \text{diag}(p_i)$  is determined by [34]

$$p_i = \begin{cases} \max(0, \frac{2(c_i - d_i)/(\mu a_i) - 2}{1 + \sqrt{1 - 4c_i d_i + 4(c_i - d_i)c_i d_i}/(\mu a_i)}), & \text{if } c_i > d_i, \\ 0, & \text{otherwise,} \end{cases} \quad (39)$$

in which  $p_i$  and  $a_i$  are the  $i$ th diagonal element of  $\mathbf{P}$  and  $\mathbf{E}^T \mathbf{E}$ , and  $\mu$  is the Lagrange multiplier to ensure

$$\text{tr}(\mathbf{E} \mathbf{P} \mathbf{E}^T) = P_t. \quad (40)$$

So, the GSVD-based initialization of  $\mathbf{Q}$  is  $\mathbf{E} \mathbf{P} \mathbf{E}^T$ . Thus, we can determine  $\mathbf{V}^{(0)}$  and  $\boldsymbol{\Lambda}^{(0)}$  from

$$\mathbf{Q}^{(0)} = \mathbf{E} \mathbf{P} \mathbf{E}^T = \mathbf{V}^{(0)} \boldsymbol{\Lambda}^{(0)} \mathbf{V}^{(0)T}. \quad (41)$$

Next, the eigenvalues and rotation angles of  $\Lambda^{(0)}$  and  $\mathbf{V}^{(0)}$  can be obtained using Algorithm 1.

The gradient-descent rotation-based method is summarized in Algorithm 2.

---

**Algorithm 2** Rotation-based Method by Gradient Descent

---

```

1: Initialize: counter for eigenvalue iterations  $n = 0$ ;
2: Initialize: step coefficient for eigenvalues  $\rho_\lambda = 0.02$ ;
3: Initialize:  $\epsilon = 10^{-4}$ ;
4: Find:  $\mathbf{V}^{(0)}$  and  $\Lambda^{(0)}$  using GSVD in (41);
5: Find:  $\boldsymbol{\theta}^{(0)} = [\theta_{12}^{(0)}, \theta_{13}^{(0)}, \theta_{23}^{(0)}]$  using Algorithm 1;
6: Find:  $\boldsymbol{\lambda}^{(0)} = [\lambda_1^{(0)}, \lambda_2^{(0)}, \lambda_3^{(0)}]$  is the diagonal of  $\Lambda^{(0)}$ ;
7: while 1 do
8:   Initialize: counter for rotation angles iterations  $k = 0$ ;
9:   Initialize: step coefficient for rotation angles  $\rho_\theta = 0.05$ ;
10:  while 1 do
11:    Update counter:  $k = k + 1$ ;
12:    Calculate:  $\nabla_{\boldsymbol{\theta}} R$  using (37a);
13:    Update rotation angles:  $\boldsymbol{\theta}^{(k)} = \boldsymbol{\theta}^{(k-1)} + \rho_\theta \nabla_{\boldsymbol{\theta}} R$ ;
14:    Calculate  $R$  using (26) and let  $R_\theta^{(k)} = R$ ;
15:    if  $0 \leq R_\theta^{(k)} - R_\theta^{(k-1)} < \epsilon |R_\theta^{(k-1)}|$  then
16:       $R_\theta^{\max} = \max(0, R_\theta^{(k)})$ ; break;
17:    end if
18:    if  $R_\theta^{(k)} > R_\theta^{(k-1)}$  then
19:       $\rho_\theta = 1.1 \rho_\theta$ ;
20:    else
21:       $\rho_\theta = 0.7 \rho_\theta$ ;
22:    end if
23:  end while
24:  Update counter:  $n = n + 1$ ;
25:  Calculate:  $\nabla_{\boldsymbol{\lambda}} R$  using (37b);
26:  Update eigenvalues:  $\boldsymbol{\lambda}^{(n)} = \boldsymbol{\lambda}^{(n-1)} + \rho_\lambda \nabla_{\boldsymbol{\lambda}} R$ ;
27:  Normalize eigenvalue  $\boldsymbol{\lambda}^{(n)}$  using (36);
28:  Calculate  $R$  using (26) and let  $R_\lambda^{(n)} = R$ ;

```

---

```

29: if  $0 \leq R_{\lambda}^{(n)} - R_{\lambda}^{(n-1)} < \epsilon |R^{(n-1)}|$  then
30:    $R^{\max} = \max(0, R_{\lambda}^{(n)})$ ; break;
31: end if
32: if  $R_{\theta}^{(k)} > R_{\theta}^{(k-1)}$  then
33:    $\rho_{\lambda} = 0.9\rho_{\lambda}$ ;
34: else
35:    $\rho_{\lambda} = 1.3\rho_{\lambda}$ ;
36: end if
37: end while
38: Output:  $R^{\max}$ ,  $\lambda^{(n)}$ , and  $\theta^{(k)}$ .

```

---

## V. NUMERICAL RESULT

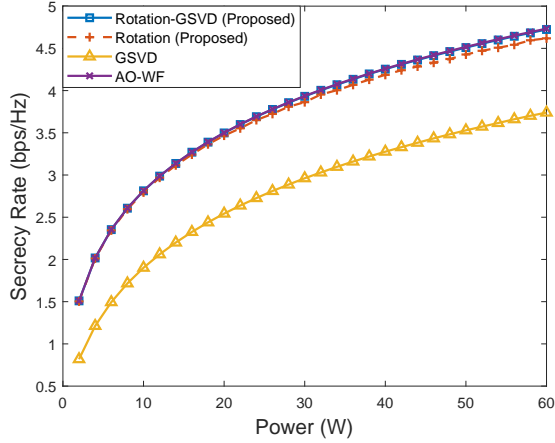
In this section, extensive numerical results are provided to illustrate the performance of the proposed method. Our results are compared with GSVD-based beamforming with optimal power allocation [34] and also the alternating optimization and water-filling (AO-WF) proposed in [12]. Two kinds of initializations are applied to the proposed rotation-based method. In the first approach, eigenvalues and rotation angles are initialized randomly (labeled by Rotation) whereas in the second approach they are initialized based on the output of GSVD-based beamforming (labeled by Rotation-GSVD). All plots are based on averaging on 100 realizations of independent  $\mathbf{H}$  and  $\mathbf{G}$ . The entries of  $\mathbf{H}$  and  $\mathbf{G}$  are generated based on the standard Gaussian distribution, i.e.,  $\mathcal{N}(0, 1)$ .

This section is divided into two subsections. In the first subsection, the case where the eavesdropper has a fewer number of antennas is discussed. Under such condition, AO-WF and the proposed method have better performance than GSVD-based beamforming. In the second subsection, the problem in AO-WF is analyzed when eavesdropper has a large number of antennas. In the end, a statistical analysis of the distribution of eigenvalues in the rotation-based method is provided.

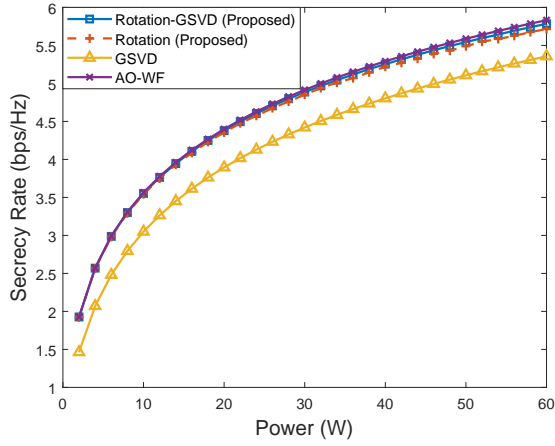
### A. MIMOME with $n_e < n_t$

In this subsection, we let  $n_t = 3$  and  $n_e = 1$ , and change  $n_r$ . The cases that the receiver has different antennas are shown in Fig. 3.

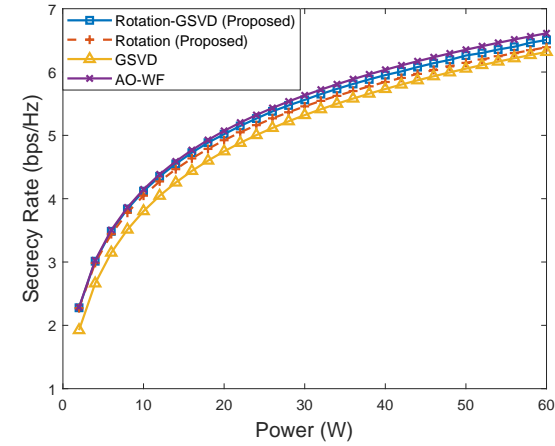
GSVD-based beamforming is relatively fast precoding and power allocation approach for the MIMOME channel. The precoding and the power allocation matrices can be obtained analytically,



(a)  $n_t = 3$ ,  $n_r = 2$ , and  $n_e = 1$



(b)  $n_t = 3$ ,  $n_r = 3$ , and  $n_e = 1$



(c)  $n_t = 3$ ,  $n_r = 4$ , and  $n_e = 1$

Fig. 3: Secrecy rate of the MIMOME channel versus the transmit power for  $n_t = 3$ ,  $n_e = 1$ , and different value of  $n_r$ . The proposed methods are compared with GSVD-based beamforming and AO-WF.

as explained in Section IV-B. However, when the eavesdropper has a smaller number of antennas than the legitimate receiver, GSVD-based beamforming fails to get close to the secrecy capacity, as can be seen in Fig. 3, and also is verified by previous literature [11]. The gap can be very large as seen in Fig. 3. Nonetheless, GSVD-based beamforming can produce effective initial values for the parameters in our proposed rotation-based method.<sup>5</sup>

The rotation-based method and AO-WF give similar results initialized by GSVD-based beamforming, and the time cost is also close. If the initial values are given randomly, the rotation-based method has about three times of higher cost compared to AO-WF, in this experiment. Meanwhile, the achievable secrecy rate is slightly lower, which means GSVD-based beamforming can give an efficient initial values for our rotation-based method.

### B. MIMOME with $n_e \geq n_r$ and Modified AO-WF

When the number of antennas at the eavesdropper is higher than or equal to the number of antennas at the receiver, AO-WF cannot use the full average power, which means  $\text{tr}(\mathbf{Q}) < P_t$  happens. Fig. 4 illustrates the ratio of the power that actually used in the solution of AO-WF, i.e.,  $\text{tr}(\mathbf{Q})/P_t$ . The result is based on 100 realizations of  $\mathbf{H}$  and  $\mathbf{G}$  when the  $n_t = 3$ ,  $n_r = 4$ , and  $n_e = 5$ .

This limitation comes from the Lagrange multiplier of AO-WF. The inner loop of AO-WF uses a binary search to find the Lagrange multiplier such that  $\text{tr}(\mathbf{Q})$  reaches the average power  $P_t$ . However, when  $n_e \geq n_t$  the first several outer-iterations cannot give a nonzero solution for the Lagrange multiplier.

To illustrate this, we apply AO-WF on following  $\mathbf{H}$  and  $\mathbf{G}$

$$\mathbf{H} = \begin{bmatrix} 1.4628 & -1.9093 & 0.2941 \\ -0.8861 & 0.9319 & 0.6151 \\ -1.9243 & 0.7442 & 0.3094 \\ -0.4729 & -1.2250 & -0.1745 \end{bmatrix}, \quad (42)$$

<sup>5</sup>We need to mention that the covariance matrix given by AO-WF may use higher power than the total average power, i.e.  $\text{tr}(\mathbf{Q}) > P_t$ . To overcome this shortcoming, we add a termination condition, i.e.,  $\text{tr}(\mathbf{Q}) - P_t \leq 10^{-6}$ , to ensure the constraints in (2) are fulfilled.

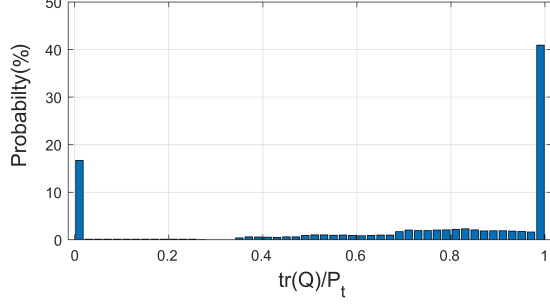


Fig. 4: The rate of power used in AO-WF.

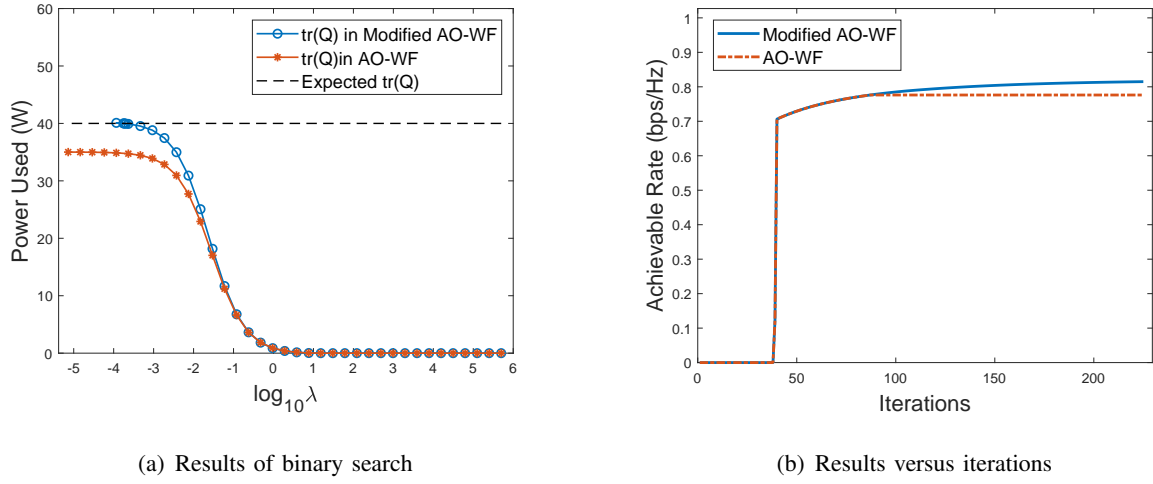


Fig. 5: Comparison of original and modified AO-WF for  $P_t = 40W$  and one realization of  $\mathbf{H}$  and  $\mathbf{G}$ .

$$\mathbf{G} = \begin{bmatrix} -2.0156 & -0.8023 & 0.1474 \\ -2.1129 & -0.3437 & 0.1646 \\ -1.5204 & -1.1948 & -0.2154 \\ -0.7177 & 1.7458 & -0.4084 \\ 0.3622 & 1.3965 & -2.1588 \end{bmatrix}. \quad (43)$$

Fig. 5(a) shows the status of binary search for Lagrange multiplier when the termination condition of AO-WF have been met (the outer loop terminates at iteration 87). The binary search gives a Lagrange multiplier  $\lambda$  close to zero ( $\approx 10^{-5}$ ), as can be seen in Fig. 5(a). That is, the binary search loses its efficacy because during the search the trace of the covariance matrix  $\mathbf{Q}$  (the

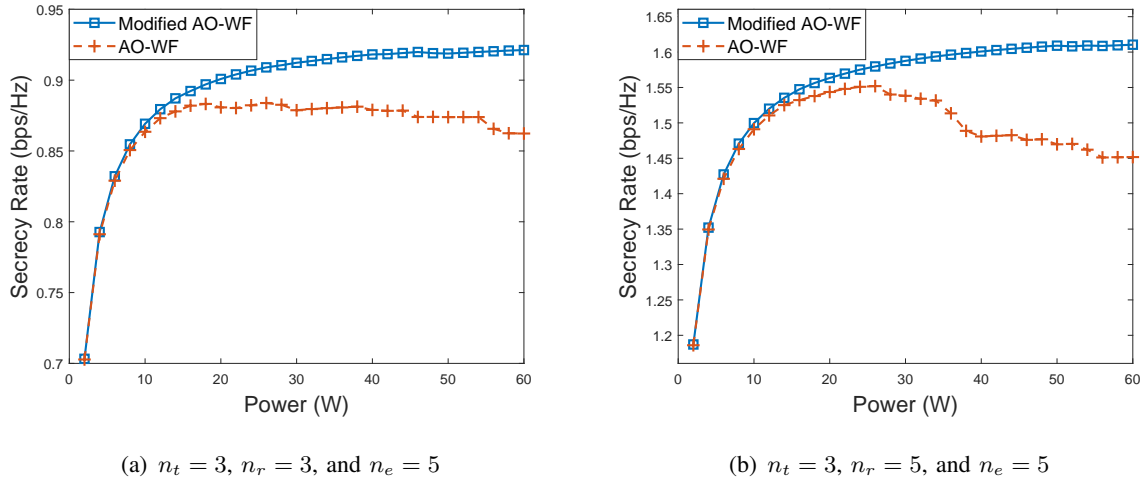


Fig. 6: Comparison between original and modified AO-WF for  $n_t = 3$ ,  $n_e = 5$ , and different  $n_r$ s.

curve with respect to AO-WF in Fig. 5(a)) has no intersection with the aimed average power  $P_t$  (the dashed line Fig. 5(a)).

A feasible solution to this problem is to increase the number of iterations for the outer loop. To this end, we modify the AO-WF algorithm by using a stricter stop condition for the outer loop. Specifically, we change the termination condition from

$$|R(\mathbf{Q}^{(n)}) - R(\mathbf{Q}^{(n-1)})| / R(\mathbf{Q}^{(n-1)}) \leq \epsilon, \quad (44)$$

to

$$\left| R(\mathbf{Q}^{(n)}) - \sum_{k=n-21}^{n-1} R(\mathbf{Q}^{(k)}) \right| / \sum_{k=n-21}^{n-1} R(\mathbf{Q}^{(k)}) \leq \epsilon. \quad (45)$$

In this new termination condition,  $R(\mathbf{Q}^{(n)})$  is compared with the average of previous 20 iterations. The curve with respect to modified AO-WF in Fig. 5(a) shows that a non-zero Lagrange multiplier is successfully found with this modification. Accordingly, the secrecy rate slightly goes up in Fig. 5(b). However, it should be noted that, as a result of this change the number of iterations of the outer loop increases from 87 to 225. That is, the modification comes at the cost of a higher computational complexity.

The aforementioned issue for the AO-WF algorithm appears when  $n_e \geq n_t$ . The proposed modified AO-WF overcomes this issue and performs better than the original one when  $n_e \geq n_t$  as

shown in Fig. 6. Modified AO-WF is also more stable and can provide a higher secrecy rate. For  $n_e \geq n_t$ , we benchmark our rotation-based algorithms with the modified AO-WF. Even with this, our precoding outperforms that algorithm. Obviously, when compared with the original AO-WF the performance gap will be higher.

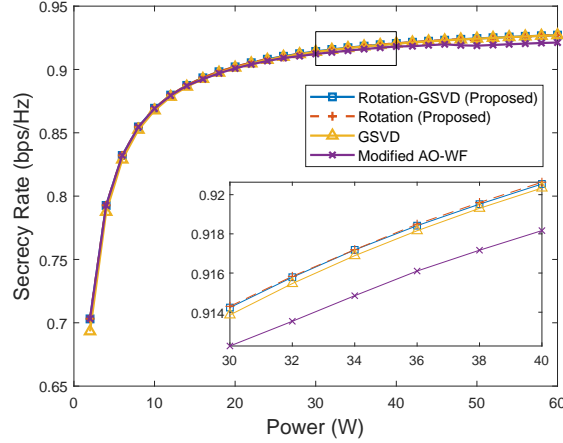
A comparison of GSVD-based beamforming, modified AO-WF, and the proposed rotation-based algorithms are illustrated in Fig. 7, where the eavesdropper has a higher number of antennas than the receiver. The rotation-based method initiated by GSVD-based beamforming shows the best performance in all three situations.

To summarize, in this section, we have examined the proposed rotation method with GSVD-based beamforming and AO-WF in the MIMOME channel for various number of antennas at each node. It turns out that when  $n_e < n_t$  both AO-WF and the proposed method achieve better secrecy rate than GSVD-based beamforming. When the eavesdropper has a higher number of antennas than the transmitter, the AO-WF faces a problem. To overcome this issue, a modification is applied to AO-WF in this section. The modified AO-WF has a better stability compared to the original one and improves the rate. Even when compared with the modified AO-WF, our proposed methods still show better performance compared to GSVD-based beamforming and modified AO-WF.

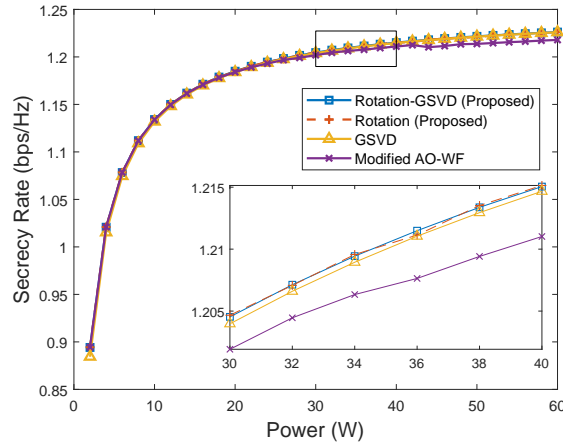
## VI. CONCLUSIONS

In this paper, we have developed a rotation-based method for precoding and power allocation of the MIMOME channel. In this method, the transmit covariance matrix is constructed using a rotation matrix, which is used as a precoder, and a power allocation matrix. With this construction, the positive semi-definite constraint of the transmit covariance matrix is removed and the capacity region optimization problem is simplified. The optimal precoding (rotation) matrix and power allocation coefficients have been obtained through the gradient descent method. Compared to existing numerical approaches, the proposed method is robust and performs well independent of the number of antennas at each node. The proposed method remarkably outperforms the GSVD-based beamforming when  $n_e = 1$ , and is slightly better than AO-WF, even we modified. This approach can also use the results of existing precoding and power allocation methods, such as GSVD-based approach, as an initial point to expedite finding the optimal solution.

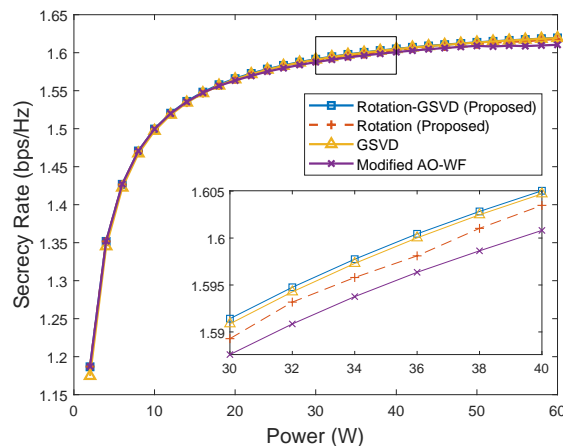
The proposed rotation-based method is efficient in the MIMOME channel. More importantly, it has a great potential for optimizing precoding and power allocation in various other applications



(a)  $n_t = 3$ ,  $n_r = 3$ , and  $n_e = 5$



(b)  $n_t = 3$ ,  $n_r = 4$ , and  $n_e = 5$



(c)  $n_t = 3$ ,  $n_r = 5$ , and  $n_e = 5$

Fig. 7: Secrecy rate of the MIMOME channel for  $n_t = 3$ ,  $n_e = 5$ , and different numbers of receive antennas. The proposed rotation-based methods are compared with GSVD-based beamforming and modified AO-WF.

including in MIMO broadcast channel, with and without secrecy. Future works will focus on simplification of solving parameters in the rotation model and extension of this approach to other related problems.

## REFERENCES

- [1] A. D. Wyner, “The wire-tap channel,” *Bell System Technical Journal*, vol. 54, no. 8, pp. 1355–1387, 1975.
- [2] U. M. Maurer, “Secret key agreement by public discussion from common information,” *IEEE Transactions on Information Theory*, vol. 39, no. 3, pp. 733–742, 1993.
- [3] I. Csiszár and J. Körner, “Broadcast channels with confidential messages,” *IEEE Transactions on Information Theory*, vol. 24, no. 3, pp. 339–348, 1978.
- [4] A. Khisti and G. W. Wornell, “Secure transmission with multiple antennas part II: The MIMOME wiretap channel,” *IEEE Transactions on Information Theory*, vol. 11, no. 56, pp. 5515–5532, 2010.
- [5] F. Oggier and B. Hassibi, “The secrecy capacity of the MIMO wiretap channel,” *IEEE Transactions on Information Theory*, vol. 57, no. 8, pp. 4961–4972, 2011.
- [6] T. Liu and S. Shamai, “A note on the secrecy capacity of the multiple-antenna wiretap channel,” *IEEE Transactions on Information Theory*, vol. 55, no. 6, pp. 2547–2553, 2009.
- [7] S. Shafiee, N. Liu, and S. Ulukus, “Towards the secrecy capacity of the Gaussian MIMO wire-tap channel: the 2-2-1 channel,” *IEEE Transactions on Information Theory*, vol. 55, no. 9, pp. 4033–4039, 2009.
- [8] P. Parada and R. Blahut, “Secrecy capacity of SIMO and slow fading channels,” in *International Symposium on Information Theory*, pp. 2152–2155, IEEE, 2005.
- [9] S. A. A. Fakoorian and A. L. Swindlehurst, “Full rank solutions for the MIMO Gaussian wiretap channel with an average power constraint,” *IEEE Transactions on Signal Processing*, vol. 61, no. 10, pp. 2620–2631, 2013.
- [10] S. Loyka and C. D. Charalambous, “Optimal signaling for secure communications over Gaussian MIMO wiretap channels,” *IEEE Transactions on Information Theory*, vol. 62, no. 12, pp. 7207–7215, 2016.
- [11] M. Vaezi, W. Shin, and H. V. Poor, “Optimal beamforming for Gaussian MIMO wiretap channels with two transmit antennas,” *IEEE Transactions on Wireless Communications*, vol. 16, no. 10, pp. 6726–6735, 2017.
- [12] Q. Li, M. Hong, H.-T. Wai, Y.-F. Liu, W.-K. Ma, and Z.-Q. Luo, “Transmit solutions for MIMO wiretap channels using alternating optimization,” *IEEE Journal on Selected Areas in Communications*, vol. 31, no. 9, pp. 1714–1727, 2013.
- [13] S. Loyka and C. D. Charalambous, “An algorithm for global maximization of secrecy rates in Gaussian MIMO wiretap channels,” *IEEE Transactions on Communications*, vol. 63, no. 6, pp. 2288–2299, 2015.
- [14] J. Steinwandt, S. A. Vorobyov, and M. Haardt, “Secrecy rate maximization for MIMO Gaussian wiretap channels with multiple eavesdroppers via alternating matrix POTDC,” in *IEEE International Conference on Acoustics, Speech and Signal Processing*, pp. 5686–5690, IEEE, 2014.
- [15] J. Li and A. Petropulu, “Transmitter optimization for achieving secrecy capacity in Gaussian MIMO wiretap channels,” *arXiv preprint arXiv:0909.2622*, 2009.
- [16] M. Vaezi, W. Shin, H. V. Poor, and J. Lee, “MIMO Gaussian wiretap channels with two transmit antennas: Optimal precoding and power allocation,” in *Proc. IEEE International Symposium on Information Theory*, pp. 1708–1712, 2017.
- [17] Y. Yang, Q. Li, W.-K. Ma, J. Ge, and P. Ching, “Cooperative secure beamforming for AF relay networks with multiple eavesdroppers,” *IEEE Signal Processing Letters*, vol. 20, no. 1, pp. 35–38, 2013.
- [18] J. Huang and A. L. Swindlehurst, “Cooperative jamming for secure communications in MIMO relay networks,” *IEEE Transactions on Signal Processing*, vol. 59, no. 10, pp. 4871–4884, 2011.

- [19] J. Li and A. P. Petropulu, "On ergodic secrecy rate for Gaussian MISO wiretap channels," *IEEE Transactions on Wireless Communications*, vol. 10, no. 4, pp. 1176–1187, 2011.
- [20] Y. Wu, C. Xiao, Z. Ding, X. Gao, and S. Jin, "Linear precoding for finite-alphabet signaling over MIMOME wiretap channels," *IEEE Transactions on Vehicular Technology*, vol. 61, no. 6, pp. 2599–2612, 2012.
- [21] W. Zeng, C. Xiao, M. Wang, and J. Lu, "Linear precoding for finite-alphabet inputs over MIMO fading channels with statistical CSI," *IEEE Transactions on Signal Processing*, vol. 60, no. 6, pp. 3134–3148, 2012.
- [22] S. R. Aghdam, A. Nooraeipour, and T. M. Duman, "An overview of physical layer security with finite-alphabet signaling," *IEEE Communications Surveys and Tutorials*, 2018.
- [23] H. Lee, C. Song, J. Moon, and I. Lee, "Precoder designs for MIMO Gaussian multiple access wiretap channels," *IEEE Transactions on Vehicular Technology*, vol. 66, no. 9, pp. 8563–8568, 2017.
- [24] D. Park, "Secrecy sum rates of MIMO multi-receiver wiretap channels," *IEEE Communications Letters*, vol. 20, no. 9, pp. 1804–1807, 2016.
- [25] S. A. A. Fakoorian and A. L. Swindlehurst, "MIMO interference channel with confidential messages: Achievable secrecy rates and precoder design," *IEEE Transactions on Information Forensics and Security*, vol. 6, no. 3, pp. 640–649, 2011.
- [26] D. Park, "Weighted sum rate maximization of MIMO broadcast and interference channels with confidential messages," *IEEE Transactions on Wireless Communications*, vol. 15, no. 3, pp. 1742–1753, 2015.
- [27] M. Vaezi and H. V. Poor, "NOMA: An Information-Theoretic Perspective," in *Multiple Access Techniques for 5G Wireless Networks and Beyond*, pp. 167–193, Springer, 2019.
- [28] B. Fang, Z. Qian, W. Shao, and W. Zhong, "Precoding and artificial noise design for cognitive MIMOME wiretap channels," *IEEE Transactions on Vehicular Technology*, vol. 65, no. 8, pp. 6753–6758, 2015.
- [29] M. A. Arfaoui, M. D. Soltani, I. Tavakkolnia, A. Ghayeb, C. Assi, M. Safari, and H. Haas, "Physical layer security for visible light communication systems: A survey," *arXiv preprint arXiv:1905.11450*, 2019.
- [30] J. Zhang, C. Yuen, C.-K. Wen, S. Jin, K.-K. Wong, and H. Zhu, "Large system secrecy rate analysis for SWIPT MIMO wiretap channels," *IEEE Transactions on Information Forensics and Security*, vol. 11, no. 1, pp. 74–85, 2015.
- [31] W. Wu and B. Wang, "Efficient transmission solutions for MIMO wiretap channels with SWIPT," *IEEE Communications Letters*, vol. 19, no. 9, pp. 1548–1551, 2015.
- [32] H. Niu, D. Guo, Y. Huang, and B. Zhang, "Robust energy efficiency optimization for secure MIMO SWIPT systems with non-linear EH model," *IEEE Communications Letters*, vol. 21, no. 12, pp. 2610–2613, 2017.
- [33] A. Khisti and G. W. Wornell, "Secure transmission with multiple antennas I: The MISOME wiretap channel," *IEEE Transactions on Information Theory*, vol. 56, no. 7, pp. 3088–3104, 2010.
- [34] S. A. A. Fakoorian and A. L. Swindlehurst, "Optimal power allocation for GSVD-based beamforming in the MIMO Gaussian wiretap channel," in *IEEE International Symposium on Information Theory Proceedings*, pp. 2321–2325, 2012.
- [35] G. G. Slabaugh, "Computing Euler angles from a rotation matrix," *Retrieved on August*, vol. 6, no. 2000, pp. 39–63, 1999.
- [36] S. Matthies, "Orientations and rotations: computations in crystallographic textures," *Journal of Applied Crystallography*, vol. 38, no. 6, pp. 1042–1043, 2005.
- [37] G. H. Golub and C. F. Van Loan, *Matrix computations*, vol. 3. JHU press, 2012.
- [38] J. R. Magnus and H. Neudecker, *Matrix differential calculus with applications in statistics and econometrics*. Wiley, 2019.